Controlling the canted state in antiferromagnetically coupled magnetic bilayers close to the spin reorientation transition

Cite as: Appl. Phys. Lett. **110**, 102405 (2017); https://doi.org/10.1063/1.4978430
Submitted: 25 November 2016 . Accepted: 28 February 2017 . Published Online: 10 March 2017

F. C. Ummelen, A. Fernández-Pacheco, R. Mansell, D. Petit, H. J. M. Swagten, and R. P. Cowburn

Controlling the canted state in antiferromagnetically coupled magnetic bilayers close to the spin reorientation transition

F. C. Ummelen,[1] A. Fernández-Pacheco,[2,a)] R. Mansell,[2] D. Petit,[2] H. J. M. Swagten,[1] and R. P. Cowburn[2]
[1]*Department of Applied Physics, University of Technology, P.O. Box 513, 5600 MB Eindhoven, The Netherlands*
[2]*Cavendish Laboratory, University of Cambridge, JJ Thomson Avenue, Cambridge CB3 0HE, United Kingdom*

(Received 25 November 2016; accepted 28 February 2017; published online 10 March 2017)

Canted magnetization is obtained in ultrathin, antiferromagnetically coupled magnetic bilayers with thicknesses around the spin reorientation transition. The canting angle is controlled by both the magnetic layer thickness and interlayer coupling strength, which are tuned independently. Hysteresis loops are obtained, where magnetization components parallel and transverse to the applied field are measured, and analyzed by comparison to micromagnetic simulations. This enables the canting angle to be extracted and the behavior of the individual layers to be distinguished. Two types of canted systems are obtained with either single-layer reversal or complex, coupled two-layer reversal, under moderate external magnetic fields. Controlling the magnetization canting and reversal behavior of ultra-thin layers is relevant for the development of magnetoresistive random-access memory and spin-torque oscillator devices. [http://dx.doi.org/10.1063/1.4978430]

The unusual situation that the magnetization of a thin film is neither out-of-plane (OOP) nor in-plane (IP) is referred to as a canted state. The first works on canted states relied on the interplay between the first and second order magnetic anisotropy.[1–3] Because the second order anisotropy is hard to control and the regime in which canted states can be found using this method is small,[4] recent works have focused on interlayer coupling to create canted states.[5,6] Non-collinear magnetizations have been reported in Ruderman-Kittel-Kasuya-Yosida (RKKY) coupled bilayer systems.[7–10] Furthermore, there have been reports on layers with in-plane and perpendicular anisotropy coupled by direct ferromagnetic exchange interactions.[11] In those cases, the canting angle can be controlled via the thickness of the magnetic layers. The measurement of canting can be carried out using x-ray magnetic circular dichroism or photoelectron emission microscopy,[7–9] which allow the different layers to be studied individually but require large and expensive facilities. Techniques such as magneto-optical Kerr effect (MOKE), vibrating sample magnetometry, or magnetoresistance measurements are also used,[6,12] but these data are not straightforward to interpret because all magnetic layers contribute to the total signal. Here, we perform a systematic study on the following system: a Pt/Co/Pt layer, antiferromagnetically coupled to a Pt/CoFeB/Pt layer via RKKY coupling through a Ru layer. In order to finely control the canting angle of the layers, we separately tune the effective perpendicular magnetic anisotropy (PMA) of both layers, as well as the antiferromagnetic RKKY interaction between them. A combination of standard magnetometry measurements and micromagnetic simulations enables us to derive the behavior of the individual layers as a function of the magnetic field, making it possible to extract their canting angle at remanence. Canted magnetic states as those shown here could be exploited in magnetic random access memory (MRAM) and spin-transfer torque oscillators. These devices could be significantly improved by the use of a polarizer with a canted magnetization, leading to an enhanced spin-transfer torque, since this effect scales with the sine of the angle between the magnetization of the two magnetic layers.[13–17]

To describe canting mathematically, we define θ as the angle between the magnetization direction and the surface normal, as indicated in Figure 1(a). The system is said to be in a canted state if in one of the layers θ is not equal to 0°, 90°, or 180°. The energy per unit area, E, of the two coupled magnetic layers is given by

$$E = K_{\mathrm{eff}1} t_1 \sin^2\theta_1 + K_{\mathrm{eff}2} t_2 \sin^2\theta_2 - J\frac{\vec{M}_1 \cdot \vec{M}_2}{|M_1||M_2|}, \quad (1)$$

where the first two terms in this equation represent the uniaxial magnetic anisotropy, with t_1 and t_2 the layer thicknesses, and $K_{\mathrm{eff}1}$ and $K_{\mathrm{eff}2}$ the first-order anisotropy constants of layers 1 and 2. These are effective anisotropy constants, defined as $K_{\mathrm{eff}} = \frac{2K_S}{t} - \frac{1}{2}\mu_0 M_S^2$. They include contributions from the two interfaces via the surface anisotropy K_S and the shape anisotropy, where M_S is the saturation magnetization. We neglect the possible difference between the two interfaces.[18] The third term in Equation (1) represents the isotropic coupling to another layer, with J the coupling surface energy (which is negative for antiferromagnetic coupling) and $\vec{M}_1$ and $\vec{M}_2$ the magnetization of the two layers.

All samples consist of ultrathin films, grown using DC magnetron sputtering, in a system with a base pressure of 9×10^{-8} mbar and a growth pressure of 8×10^{-3} mbar. The structure investigated (see Fig. 1) is Ta(4.0 nm)/Pt(10.0 nm)/

a)af457@cam.ac.uk

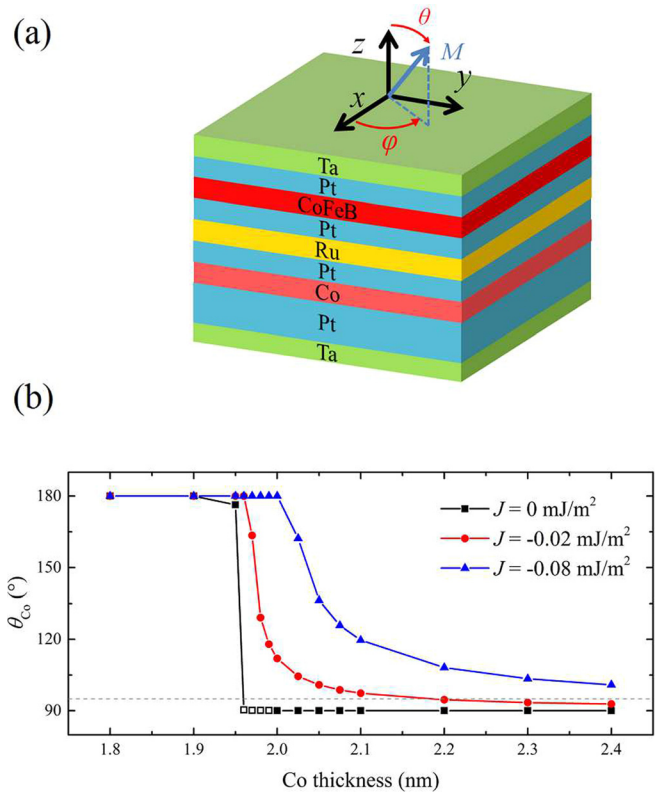

FIG. 1. (a) Schematic representation of the investigated bilayers and the definition of the coordinate system. (b) Micromagnetic simulations of the behavior of a Co layer of varying thickness (horizontal axis) for different strengths of coupling to a 0.6 nm CoFeB layer with perpendicular magnetic anisotropy. $K_S = 1.2$ mJ/m^2 and $K_S = 0.7$ mJ/m^2 are the surface anisotropy constants used for Co and CoFeB, respectively. Closed (open) symbols represent monodomain (multidomain) states. The θ angles associated to states with multiple domains correspond to effective angles, calculated by averaging x and z components of the total magnetisation of the Co layer. Without RKKY coupling, the SRT is abrupt and includes multidomain states. With RKKY coupling to an out-of-plane layer, the SRT becomes continuous and no multidomain states are observed. See details of these simulations in videos 1–3, supplementary material.

Co(x nm)/Pt(y nm)/Ru(1.0 nm)/Pt(y nm)/CoFeB(z nm)/Pt(2.0 nm)/Ta(2.0 nm). The anisotropy constant of each layer depends on its thickness, and varying this thickness is used to tune the proximity of the layers with respect to the spin reorientation transition (SRT), the regime in which the anisotropy changes from out-of-plane to in-plane.[19] The thicknesses of the magnetic layers were varied from 0.6 nm to 2.0 nm (x) and from 2.0 to 2.2 nm (z). The magnetic layers are coupled via RKKY coupling, and the Ru thickness of 1.0 nm is chosen to be at the first antiferromagnetic peak. The strength of the coupling can be finely tuned by the thickness of the Pt at the Ru interface,[20] y is 0.5 nm or 0.7 nm, which results in a coupling constant of -0.08 mJ/m^2 or -0.02 mJ/m^2, respectively. We verified experimentally (supplementary material S1) that the coupling constants are the same for in-plane magnetized or out-of-plane layers, which could be not the case due to the possible different density of states for the two configurations.[21]

Measurements are performed in a vibrating sample magnetometer (VSM). External magnetic fields are applied along different directions, and the components of the magnetization both along the field direction and transverse to it are measured using two sets of pick-up coils. In particular, we apply fields along the direction corresponding to the hard axis of the layer which is further from the SRT, which is key to understanding the magnetic behavior of the system, and therefore, to extracting the canting angle of the layers at remanence. Additional experiments were performed using longitudinal and polar magneto-optical Kerr effect (MOKE) measurements, of which some results are shown in the supplementary material. The range of thicknesses and anisotropies for which canted states are obtained is narrow, an example of a system with no canted state is included in supplementary material S2. In the main article, we will focus on particular bilayers, which show canted states, and demonstrate the usefulness of our analysis method.

The simulations are carried out by micromagnetic simulations using Mumax3;[22] details on the parameters used can be found in supplementary material S3. This allowed us to numerically study the extended films, by fixing periodic boundary conditions. In order to check the accuracy of Mumax3 to model canted states as those investigated here, characterized by large angles between layers, we ran additional OOMMF simulations in a macrospin form,[23] finding good agreement between both types of simulations. See supplementary material S4 for more details about parameters used in the simulations and comparison between both methods.

We first measure the SRT of uncoupled Pt/Co/Pt and Pt/CoFeB/Pt layers by varying their thickness and find them to be at 1.9 nm and 1.5 nm, respectively, see supplementary material S5. As the demagnetizing energy and PMA compensate each other at the SRT, the surface anisotropy can be deduced, giving $K_S = 1.2$ mJ/m^2 and $K_S = 0.7$ mJ/m^2 for Pt/Co/Pt and Pt/CoFeB/Pt, respectively, which is comparable with values previously reported.[18,20] Using these values, we study the influence of additional energy terms on the SRT of a single layer of Pt/Co/Pt by simulations. When no second order anisotropy or coupling is present, the transition from out-of-plane to in-plane is abrupt and includes multidomain states[4] (open symbols). A second order anisotropy constant would smear out the otherwise abrupt SRT transition as a function of thickness (not shown here), but as mentioned before, we are not able to experimentally control this higher order anisotropy. By introducing antiferromagnetic coupling between the layers, the transition from OOP to IP also becomes gradual, but now in a controlled manner, shown in Figure 1(b). Moreover, the RKKY antiferromagnetic coupling to a strongly anisotropic perpendicular layer favors a single-domain state during the SRT.[24]

The first type of canted state is obtained in samples formed by an out-of-plane layer with strong PMA (0.6 nm CoFeB) and a layer close to the SRT (2.1 nm Co), strongly antiferromagnetically coupled (-0.08 mJ/m^2). Figure 2(a) shows the experimental hysteresis loops of this sample when in-plane fields are applied. Both magnetization components along the field direction, M_x, and transverse to that, M_z, are measured. When in-plane fields are applied, the z component is gradually reduced. The x component switches at small in-plane fields and shows a small coercivity. We reproduce the experimental behavior of the system for x-fields using micromagnetic simulations (Figure 2(b)). Figure 2(c) shows the angles of the magnetization (as defined in Figure 1(a)) of the

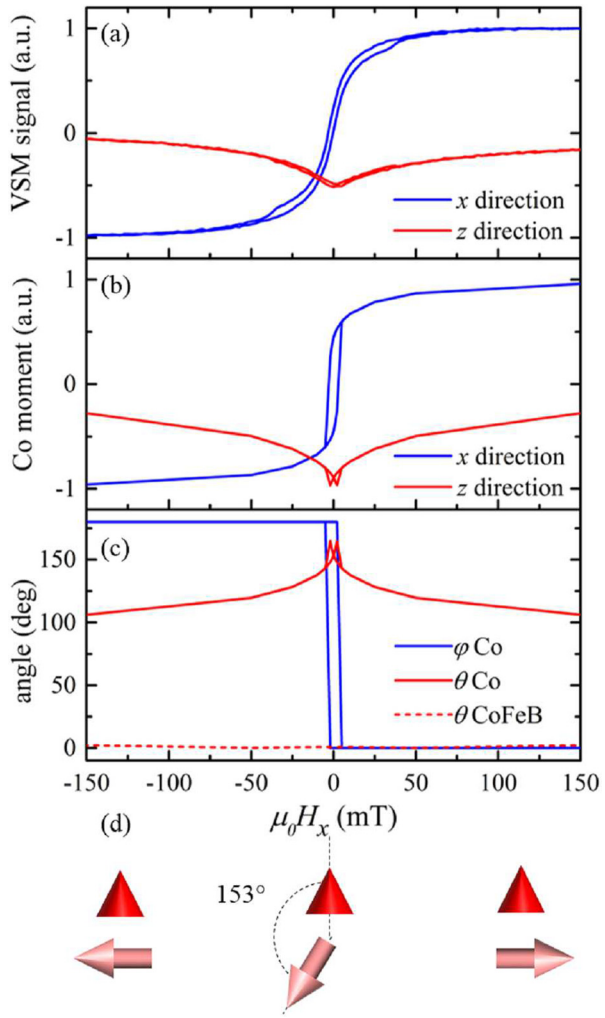

FIG. 2. (a) Hysteresis loops of a bilayer system for which the in-plane layer is canted. The magnetic field is applied along the hard axis of the uncanted layer. (b) Micromagnetic simulation of this system. (c) Behavior of the individual layers according to simulation. (d) The arrow (cone) represents the configuration of the Co (CoFeB) layer going from negative to positive fields. See details of this simulation in video 4, supplementary material.

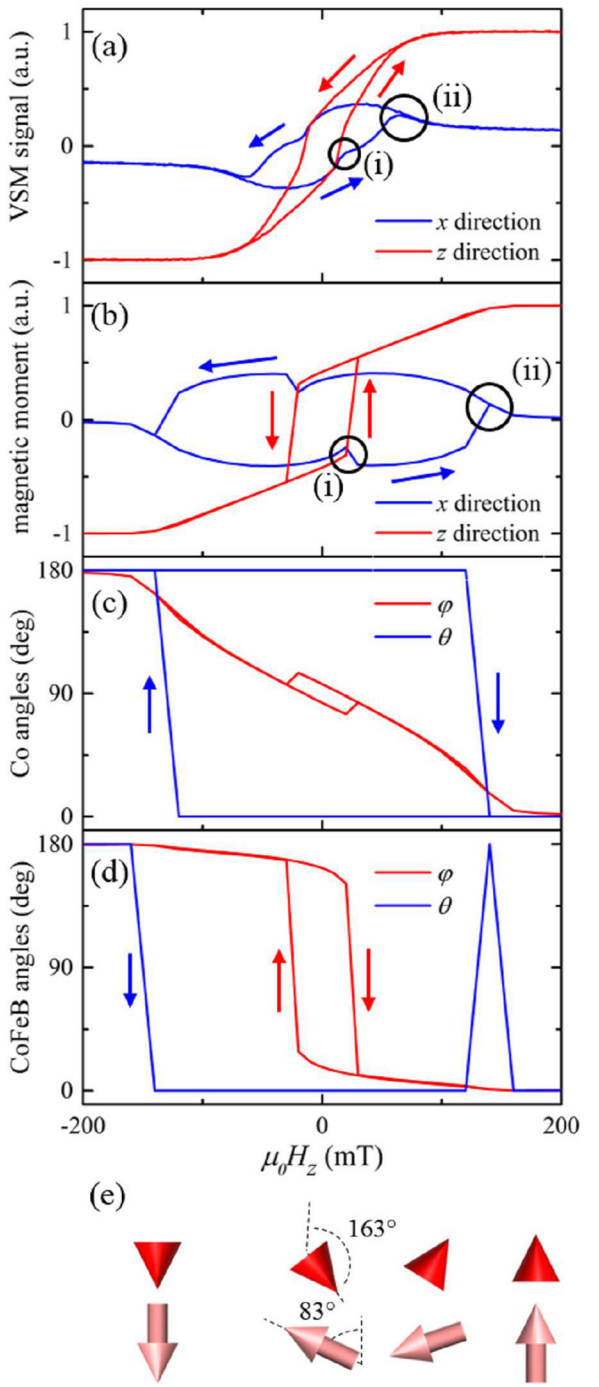

FIG. 3. (a) Hysteresis loops of a bilayer system for which both layers are canted. The magnetic field is applied along the z axis. (b) Simulation of the total magnetic moment in x and z directions. θ and the in-plane angle ϕ of the magnetization of the individual (c) Co (d) CoFeB layer. (e) The arrow (cone) indicates the configuration of the Co (CoFeB) layer going from negative to positive fields. See details of this simulation in video 5, supplementary material.

individual layers in the simulation, where $\theta = 0°$ and $\theta = 180°$ correspond to a magnetization in the $+z$ and $-z$ direction, respectively. The in-plane component is maximal when $\theta = 90°$ and points in the $+x$ direction when $\phi = 0°$. The simulations reveal that the CoFeB layer remains out-of-plane for all applied fields, as can be seen from the dashed red curve. This implies that all features in the loops come from the Co layer. At remanence, this layer is canted with $\theta \approx 153°$ according to simulations, and when fields are applied in the $\pm x$ direction, its magnetization is gradually pulled into the field direction. The configuration of the system during the measurement is schematically shown in Figure 2(d).

Whereas for this first type of canted state, only one layer changes its orientation, while the other layer remains fixed, we will now discuss the second type of canted state, for which both layers simultaneously change. These samples consist of 2.2 nm Co, 1.6 nm CoFeB and Pt thickness at the Ru interfaces that result in a weak antiferromagnetic coupling of -0.02 mJ/m^2. As shown in Figure 3(a), an interesting behavior is observed for fields along the z-direction. Although the z component of the magnetization could be explained as a combination of an easy axis and hard axis loop of two uncoupled layers, the x component reveals a more complex behavior.

Two remarkable features are highlighted: (i) a "kink" in the x component and (ii) the x component "overshoots" its equilibrium value before reaching saturation. The behavior of the system, including these features, is well reproduced by micromagnetic simulations, see Figure 3(b). The discrepancy

in switching fields can be understood due to the thermally activated nature of the switching process, which cannot be reproduced by simulations performed at 0 K. We note that the x component of the magnetization in the simulation is significantly larger than in the measurements, but this can be explained by the fact that we may not measure the complete in-plane component; the magnetization may have a component in the y direction as well. The behavior of the individual layers according to the simulations is shown in (c) and (d). For large H_z, the magnetization of both layers is aligned with the field. When this field is reduced, the Co layer becomes more in-plane, and at remanence $\theta \approx 83°$, so according to simulations the Co layer is canted 7° from the in-plane direction for zero fields. The CoFeB magnetization also rotates away from the surface normal for smaller fields because of its coupling to the Co layer. However, at remanence it still has a sizable out-of-plane component, $\theta \approx 163°$, implying that it is also canted. At an applied field of 10 mT, switching of M_z is experimentally observed, which according to the simulation is mainly due to a change in the CoFeB magnetization direction. In the simulation, the CoFeB rotates via the in-plane direction opposite to the in-plane component of the magnetization in the Co layer, because of the antiferromagnetic coupling. This results in a kink in the total x component when the CoFeB layer transits abruptly through the x-y plane (Fig. 3(d)), which explains feature (i). The second feature is reproduced by the model when a small misalignment of the magnetic field with respect to the sample normal is added in the simulations, resulting in a small additional in-plane component of the applied field. Around a field of 100 mT, the Co layer is pulled almost out-of-plane and the energy barrier for changes in the in-plane angle, ϕ, becomes very small. Therefore the small misalignment field is sufficient to switch the in-plane direction of the Co layer from 180° to 0° (Fig. 3(c)), increasing the total magnetic moment along the x-direction, which decreases again, but moderately, for larger z-fields. This gives rise to the (ii) "overshoot" feature (Fig. 3(b). In the simulations, the in-plane angle of the CoFeB layer switches around that field between 0° and 180° (for clarity, in Fig. 3(d) only the ϕ while H_z is swept from negative to positive is shown), but because the layer is almost perfectly OOP at these fields (note that θ is very close to zero), this means that there is hardly any change in the magnetization direction of that layer.

The two canted states discussed in this work are fundamentally of two different types: hard (OOP)—soft (IP) and soft (OOP)—soft (IP). A very different reversal mechanism of the magnetization is observed for these two types of systems under moderate fields. In the first case, the orientation of the OOP magnetization only changes in the IP Co layer when moderate fields are applied along the hard axis direction of the CoFeB layer, while for the second case both magnetizations reverse in a complex manner along the whole space for similar applied fields, which is consequence of their antiferromagnetic coupling and their different but close vicinity to the SRT. This key difference should be taken into account when designing devices with canted magnetized polarizers, if the approach shown here is followed.

The simulations capture the main features observed experimentally, including approximated switching field values, shape, and relative magnitude of the magnetization components. They also show that a macrospin representation of the layers for the two types of canted states discussed may be possible. This is the case when at least one of the two layers is far enough from the SRT; the antiferromagnetic RKKY coupling then favors a monodomain state in both layers[24] for hysteresis loops as those used here. Supplementary material includes an additional example of a simulation (video 6) where this is not the case: with both layers very close to the SRT, the switching occurs via a multidomain state.

In summary, we present a study on canted states in sputter deposited ultrathin magnetic layers close to the SRT, coupled via RKKY interactions for which the strength was finely tuned. We obtain two different types of canted states. The method followed here, consisting of measuring two magnetization components while applying fields along the hard axis of the layer which is further from the SRT, provides a powerful tool to analyze the complex behavior of canted states in magnetic bilayers.

See supplementary material for further details about experimental and numerical study covered in the main manuscript. See videos 1–3 for simulations of the SRT for zero, low, and high RKKY couplings. See videos 4 and 5 for simulated hysteresis loops of the two canted states. See video 6 for simulated hysteresis loop of a bilayer where the macrospin approximation is not fulfilled.

We would like to acknowledge Reinoud Lavrijsen and Dédalo Sanz-Hernández for fruitful discussions. This research was funded by the FP7 ERC 3SPIN Advanced Grant and by a European Erasmus Mobility program. This work is part of the research programme of the Foundation for Fundamental Research on Matter (FOM), which is part of the Netherlands Organisation for Scientific Research (NWO). A. Fernández-Pacheco acknowledges support from an EPSRC Early Career Fellowship EP/M008517/1, and from the Winton Foundation.

In order to comply with EPSRC policy on research data, all metadata associated to this publication can be accessed via https://doi.org/10.17863/CAM.6484.

[1]E. Y. Vedmedenko, H. P. Oepen, and J. Kirschner, J. Appl. Phys. **89**, 7145 (2001).
[2]R. Stamps, L. Louail, M. Hehn, M. Gester, and K. Ounadjela, J. Appl. Phys. **81**(8), 4751 (1997).
[3]H. Stillrich, C. Menk, R. Frömter, and H. Oepen, J. Appl. Phys. **105**(7), 07C308 (2009).
[4]M. Kisielewski, A. Maziewski, M. Tekielak, J. Ferré, S. Lemerle, V. Mathet, and C. Chappert, J. Magn. Magn. Mater. **260**, 231 (2003).
[5]A. Taga, L. Nordström, P. James, B. Johansson, and O. Eriksson, Nature **406**, 280 (2000).
[6]F. Yildiz, M. Przybylski, and J. Kirschner, Phys. Rev. Lett. **103**, 147203 (2009).
[7]C. Won, Y. Wu, H. Zhao, A. Scholl, A. Doran, and Z. Qui, Phys. Rev. B **68**, 052404 (2003).
[8]J. Choi, B.-C. Min, J.-Y. Kim, B.-G. Park, J. H. Park, Y. S. Lee, and K.-H. Shin, Appl. Phys. Lett. **99**, 102503 (2011).
[9]W. Kuch, X. Gao, and J. Kirschner, Phys. Rev. B **65**, 064406 (2002).
[10]A. Fernández-Pacheco, F. C. Ummelen, R. Mansell, D. Petit, J. H. Lee, H. J. M. Swagten, and R. P. Cowburn, Appl. Phys. Lett. **105**, 092408 (2014).
[11]T. N. A. Nguyen, R. Knut, V. Fallahi, S. Chung, Q. T. Le, S. M. Mohseni, O. Karis, S. Peredkov, R. K. Dumas, C. W. Miller, and J. Åkerman, Phys. Rev. Appl. **2**, 044014 (2014).

[12]M. Hille, A. Frauen, B. Beyersdorff, A. Kobs, S. H. Frömter, and H. Oepen, J. Appl. Phys. **113**, 023902 (2013).
[13]R. Sbiaa, R. Law, E. Tan, and T. Liew, J. Appl. Phys. **105**(1), 013910 (2009).
[14]C. Chappert, A. Fert, and F. N. V. Dau, Nat. Mater. **6**, 813 (2007).
[15]U. Roy, H. Seinige, F. Ferdousi, J. Mantey, M. Tsoi, and S. K. Banerjee, J. Appl. Phys. **111**, 07C913 (2012).
[16]Y. Zhou, C. Zha, S. Bonetti, J. Persson, and J. Åkerman, Appl. Phys. Lett. **92**, 262508 (2008).
[17]Y. Zhou, C. Zha, S. Bonetti, J. Persson, and J. Åkerman, J. Appl. Phys. **105**, 07D116 (2009).
[18]S. Bandiera, R. Sousa, B. Rodmacq, and B. Dieny, IEEE Magn. Lett. **2**, 3000504 (2011).
[19]H. Oepen, M. Speckmann, Y. Millev, and J. Kirschner, Phys. Rev. B **55**, 2752 (1997).
[20]R. Lavrijsen, A. Fernández-Pacheco, D. Petit, R. Mansell, J. H. Lee, and R. P. Cowburn, Appl. Phys. Lett. **100**, 052411 (2012).
[21]J. D. Burton and E. Y. Tsymbal, Phys. Rev. B **93**, 024419 (2016).
[22]A. Vansteenkiste, J. Leliaert, M. Dvornik, M. Helsen, F. Garcia-Sanchez, and B. V. Waeyenberge, AIP Adv. **4**, 107133 (2014).
[23]M. Donahue and D. Porter, *OOMMF User's Guide Version 1.0, Tech. Rep.* (National Institute of Standards and Technology, Gaithersburg, MD, 1999).
[24]R. R. Gareev, V. Zbarsky, J. Landers, I. Soldatov, R. Schäfer, M. Münzenberg, H. Wende, and P. Grünberg, Appl. Phys. Lett. **106**, 132408 (2015).